*Citation:* Ribeiro, A.C., Santos, L., Cerqueira Dos Santos, P., Almeida, R., Mendes, R., Conceição Mendes, A., 2022. Distribution and provenance of heavy minerals from recent sediments of Green Lake, North Brazil. Geologica Acta, 20.5, 1-14.
DOI: 10.1344/GeologicaActa2022.20.5

**geologica acta**

# Distribution and provenance of heavy minerals from recent sediments of Green Lake, North Brazil, revisited with multivariate and geostatistical analysis

**Anne Caroline S. Ribeiro[1] Livaldo O. Santos[1] Paulo Cerqueira Dos Santos[2] Rodolfo M. Almeida[1] Rodrigo C. Mendes[3] Anderson Conceição Mendes[4*]**

**[1]Universidade Federal Oeste do Pará - UFOPA, Campus Tapajós**
Rua Vera Paz, S/N, Salé - Santarém/PA, Brasil. Anne.souri@gmail.com

**[2]Faculdade de Estatística, Instituto de Ciências Naturais e Exatas, Universidade Federal do Pará-UFPA, Campus Universitário do Guamá**
Rua Augusto Correa, 01, Belém/PA 66075-110, Brasil

**[3]Programa de Pós-Graduação em Matemática, Pontifícia Universidade Católica - PUC,**
Rua Marquês de São Vicente, 225 - Gávea, Rio de Janeiro/RJ, Brasil

**[4]Faculdade de Geologia, Instituto de Geociências, Universidade Federal do Pará-UFPA, Campus Universitário do Guamá,**
Rua Augusto Correa, 01, Belém/PA 66075-110, Brasil. https://orcid.org/0000-0002-6205-6486

*Corresponding author https://orcid.org/0000-0002-6205-6486

## ABSTRACT

Geostatistical and multivariate statistical analyses were applied to heavy mineral data from an Amazonian fluvial-lake system near the Tapajós River mouth to investigate the spatial distribution and source-area of sediments. Twenty-one points were investigated, and the physical characteristics of the Green Lake deepest point were determined. Sand accumulates in the lake margins and mud quantity increases towards the lake center. Heavy mineral assemblage is composed of zircon, tourmaline, kyanite, rutile, staurolite, anatase, sillimanite, garnet, and spinel. Tourmaline, staurolite, and spinel are more abundant in the southeast area of the lake, while kyanite is dominant in the north area and zircon is in the whole lake except in its southeast area. Zircon - tourmaline and zircon - staurolite pairs are negatively correlated (r= -0.947 and -0.775, respectively), while tourmaline - staurolite and sillimanite - anatase pairs have a positive correlation (r= 0.628 and 0.675, respectively) which indicate different source rock types. Geostatistical analysis grouped the heavy minerals in three grups: Group 1 (tourmaline – staurolite – spinel - kyanite) and Group 2 (garnet – rutile – sillimanite - anatase) related to metamorphic source rocks ranging from medium to high grade, and Group 3 (zircon) related to acid igneous source rocks. The heavy mineral assemblage of Green Lake is analogous to the assemblage of the Alter do Chão Formation, indicating that this formation is the source of sediments of Green Lake.

**KEYWORDS** | **Sediment provenance. Heavy minerals. Geostatistical modeling. Green Lake.**

## INTRODUCTION

The study of the spatial distribution and composition of recent sediments is common in oceanographic re-search, as well as in studies of estuaries, lakes and modern fluvial environments (Brito *et al.*, 2009; Dadalto and Albino, 2009; Leandro *et al.*, 2014; Tavares *et al.*, 2010; Veronez Jr. *et al.*, 2009). In Amazonian sys-tems, this technique is used to understand the source and transportation of suspended load sediments (Guyot *et al.*, 2007; Viers *et al.*, 2008) and dissolved solids (Moquet *et al.*, 2016). However, only a few studies focus on the provenance of sand in lake environments (*e.g.* Sawakuchi *et al.*, 2018).

Studies of heavy minerals in recent sediments are commonly conducted to understand fluvial dynamics (Landim *et al.*, 1983; Pan *et al.*, 2016; Yang *et al.*, 2009) although it is traditionally used in provenance (Mendes *et al.*, 2015; Moral Cardona *et al.*, 2005; Morton and Hallsworth, 1994, 1999), coastal dynamic (Nascimento Jr. *et al.*, 2017; Sousa *et al.*, 2017) and stratigraphic analyses (Góes *et al.*, 2007; Knox *et al.*, 2007; Svendsen and Hartley, 2002).

Multivariate statistics have a great application in sciences, especially in environmental sciences. It is used for grouping and differentiation of n-groups (Ebqa'ai and Ibrahim, 2017; Matiatos, 2016; Yıldırım and Tokalıoğlu, 2016). It is employed for interpolation using a spatial correlation function data without bias and with minimal variance (Vieira, 2000). Despite its efficiency, its application in determining heavy mineral distributions is limited (Aguiar Neto *et al.*, 2016; Ochoa *et al.*, 2013).

Regions having different relief and erosion rates composed of different Precambrian to Cenozoic rocks are drained by Brazilian Amazon rivers (Tassinari *et al.*, 2000; Wittmann *et al.*, 2011). Hence, mixing of sediments along these rivers is common, which makes it difficult to ascertain sediments source and distribution.

Determination of spatial distribution of heavy minerals along rivers and lakes is a difficult task (Aguiar Neto *et al.*, 2016; Derkachev and Nikolaeva, 2007; Frihy *et al.*, 2022; Nascimento Jr. *et al.*, 2015; Nascimento Jr. *et al.*, 2017). Studies of geospatial distribution of heavy minerals in the Brazilian Amazon are sparse. This research aims at testing the application of multivariate techniques in the Green Lake sediments.

Heavy minerals in the Amazon River are of immature Andean origin (Landim *et al.*, 1983) whereas the ultrastable mineral assemblage of the Tapajós River interpreted as cratonic (Gozzi, 2019). In the Green Lake, sediments of the Amazon River and the Tapajós River, are mixed (Mendes *et al.*, 2020), which makes it difficult the determination of the source and the heavy mineral spatial distributions. The main objective of this research is to determine the spatial distribution of the heavy minerals in order to assess their provenance and testing the applicability of multivariate and geostatistical analysis.

## GEOLOGICAL SETTING

The Green Lake micro-basin is formed at the Tapajós and Amazon rivers' confluence due to the seasonal dis-charge variations of these rivers (Fig. 1A-C). The monthly average discharge varies from 4,000 to 30,000m$^{-3}$s$^{-1}$ in the Tapajós River and from 105,000 to 235,000m$^{-3}$s$^{-1}$ in the Amazon River (ANA, 2018). Differences in the discharge of these two rivers creates a hydraulic barrier at the mouth of the Tapajós River. This bar prevents the suspended load sediments of the Tapajós River to enter the Amazon River (Meade *et al.*, 1991).

The changes in the flow rates of the Tapajós and the Amazon rivers are due to the seasonal variations in rain-fall, which is characteristic of tropical regions. When the Amazonian rainfall period is short, the Green Lake becomes hydrologically isolated from the Tapajós River (Fig. 1E). On the other hand, if precipitation increas-es, the discharge of the Tapajós River increases, and it incorporates the Green Lake area resulting in both rivers behaving as a unified fluvial system (Fig. 1F). In such situations, as sediment distribution along rivers depends on the rock and soil types, vegetation cover, declivities, topography and rain regime, it becomes difficult to comprehend the sedimentary processes occurring within the Green Lake (Carvalho, 2008).

Cretaceous siliciclastic rocks of the Alter do Chão Formation have been considered the probable source of the heavy minerals of Green Lake (Mendes *et al.*, 2020; Ribeiro *et al.*, 2017). However, these researches failed to demonstrate a preferred spatial distribution of its heavy minerals and a relation between the Green Lake bottom sediments and the ones from the Amazon River or the Tapajós River.

## MATERIALS AND METHODS

A planimetric map with the spatial distribution of the sampling points was used (Fig. 1C). Graduated rules and Secchi discs measurements were performed to determine the lake depth. A Van Veen Grab sampler was used to collect 21 sediment samples. These samples were sieved and divided into mud and sand fractions. Green Lake's physical parameters were measured using an OAKTON multiparameter meter.

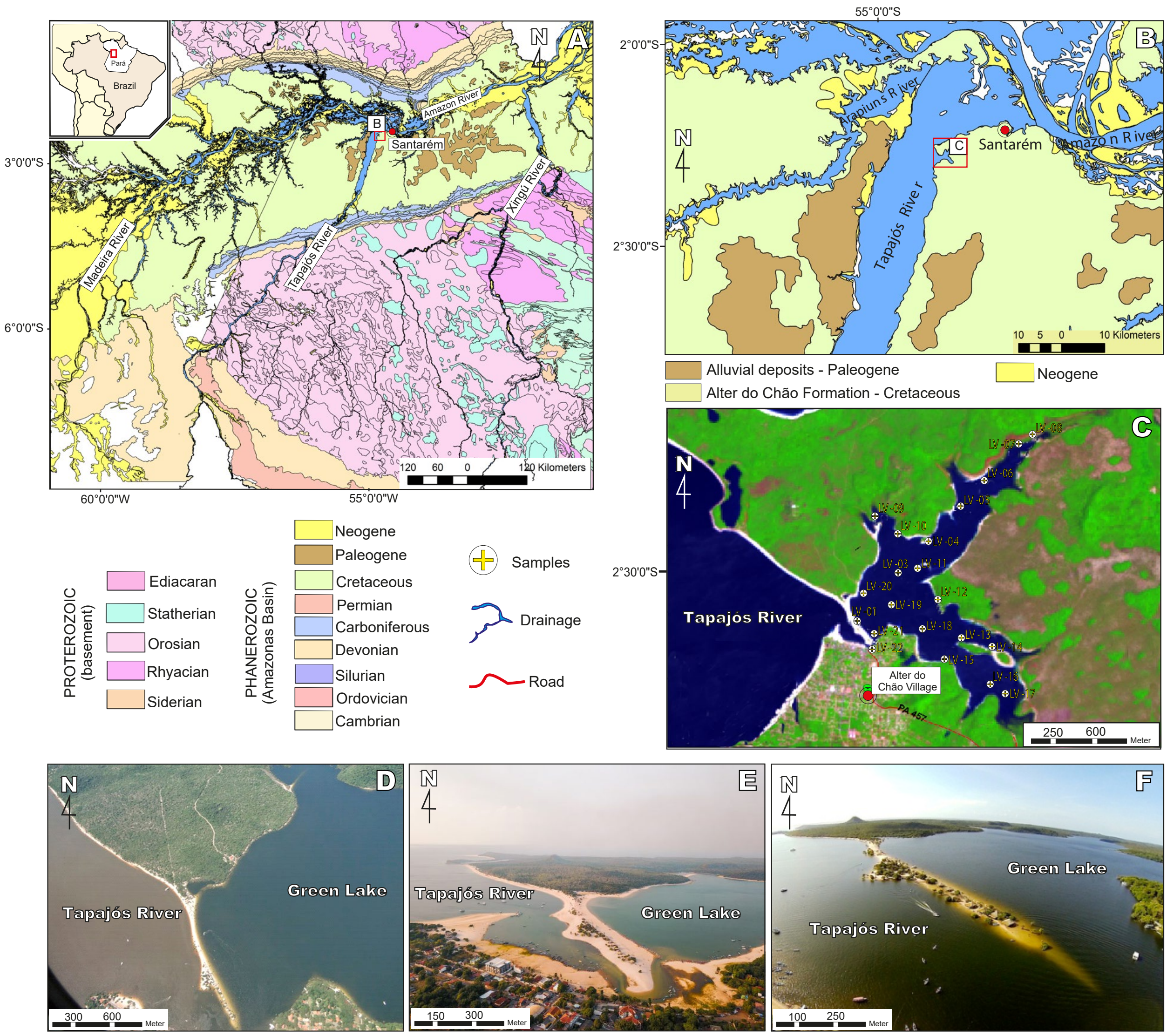


**FIGURE 1.** A-B) Geological map of the Pará State; C) map of Green Lake showing the distribution of the sampling points (Adapted from Mendes *et al*. 2020; fig. 1 B therein); D) aerial photograph of the Green Lake and Tapajós River separated by a sand bar (Love island); E) Green Lake and Tapajós River during the low rainfall period; F) Tapajós River flowing into the Green Lake during the high rainfall period.

The heavy minerals were extracted from the very fine- to fine-sized sand (63-125$\mu$m) –as most of the heavy minerals occur in this size interval (Morton and Hallsworth, 1999)– with bromoform. The heavy minerals were identified, characterized and quantified under polarized microscope based on the count of a minimum of 300grains/line (Galehouse, 1971). The Zircon-Tourmaline-Rutile (ZTR) index (Hubert, 1962) was used to determine the mineralogical maturity.

Geospatial concentration maps were constructed using the SURFER® software (Golden Software) through a kriging algorithm for interpolating data points. The kriging tool was chosen because it guarantees an excellent trend description and represents the best choice when the number of observations is limited, as in this case.

The multivariate statistical analysis was done using the SPSS software (SPSS Inc., Chicago, IL, USA). Correlation matrices were used to identify heavy mineral relations. In this analysis, Pearson's product-moment correlation coefficient (r) was applied. The Principal Component

Analysis (PCA) was used to group heavy minerals and to assess the composition of their source rocks. The PCA components were transformed using varimax rotation with Kaiser normalization.

PCA has been successfully used in the identification of pollutants. Different applications for the PCA use available data and require no factor weighting (Lu *et al.*, 2010; Tokalıoğlu and Kartal, 2006; Yongming *et al.*, 2006). Due its applicability and excellent results, PCA was applied to heavy mineral data (Cascalho, 2019; Derkachev and Nikolaeva, 2007; Ryan *et al.*, 2007).

Different heavy mineral associations were identified by Cluster analysis (Derkachev and Nikolaeva, 2007; Ryan *et al.*, 2007). The similarity measurement used in the cluster analysis was performed according to Ward's method, as this methodology agglomerates observations in different homogeneous groups with minimum variances. The results are displayed as a dendrogram created with hierarchical clustering, and the values of the distance between clusters are presented.

## RESULTS

The Green Lake is V-shaped with two arms oriented in NE-SW and NW-SE directions. It is deepest at the confluence (5.5m). The lake bottom is relatively flat and slightly deeper at the center (Fig. 2A). Sand accumulation takes place mainly in the marginal portions of the lake with grain size decreasing towards the lake center (Fig. 2B), where there is predominantly mud accumulation (Fig. 2C). In the deepest point of the lake (LV-19), physical-chemical parameters show low variation (Table 1). The measured ranges are 0.5°C for temperature, 0.71mg/L for dissolved oxygen, 0.74$\mu$S for electrical conductivity, 0.53 Nephelometric Turbidity Units (UNT) for turbidity, and 0.27 for pH.

### Heavy Minerals

Zircon, tourmaline, kyanite, rutile, staurolite, anatase, sillimanite, garnet, and spinel form the heavy minerals assemblage (Mendes *et al.*, 2020, Table 1B therein, see also their fig. 4) (Table 2; Fig. 3). This assemblage is considered moderate to stable even though the calculated ZTR index value, above 90%, indicates an abundance of stable heavy minerals (Mendes *et al.*, 2020). Mineralogical similarities, variations in spatial distribution, and significant changes in the heavy mineral assemblage were noted

The range of variation is more significant for zircon (68.1–90.2%), tourmaline (3.2–22.2%), and staurolite (0.5–6.4%) as standard deviation values are greater than 1.5. For the other heavy minerals, the variations are insignificant and the standard deviation values are less than 1.0 (Table 2).

The zircon grains are prismatic bipyramidal in shape. They are characterized by slightly worn facets, inclusions, and zoning. Tourmaline grains are subangular to rounded, having equidimensional prismatic shapes. The kyanite grains are irregular prisms presenting impact and spearhead dissolution marks. The angular staurolite grains show impact and dissolution marks. The sillimanite grains are colorless and prismatic. Garnets and spinel grains occur in a few samples, constituting up to 0.5%. They commonly show corrosion features.

### Geostatistical Analysis

The heavy mineral distribution maps (Fig. 4) show that tourmaline, staurolite, and spinel grains occur in larger quantities in the southeastern part of the lake; anatase and sillimanite grains predominate in the southeastern and northern regions; whereas the zircon grains are most present in the north-central region. The other minerals do not show a preferential distribution.

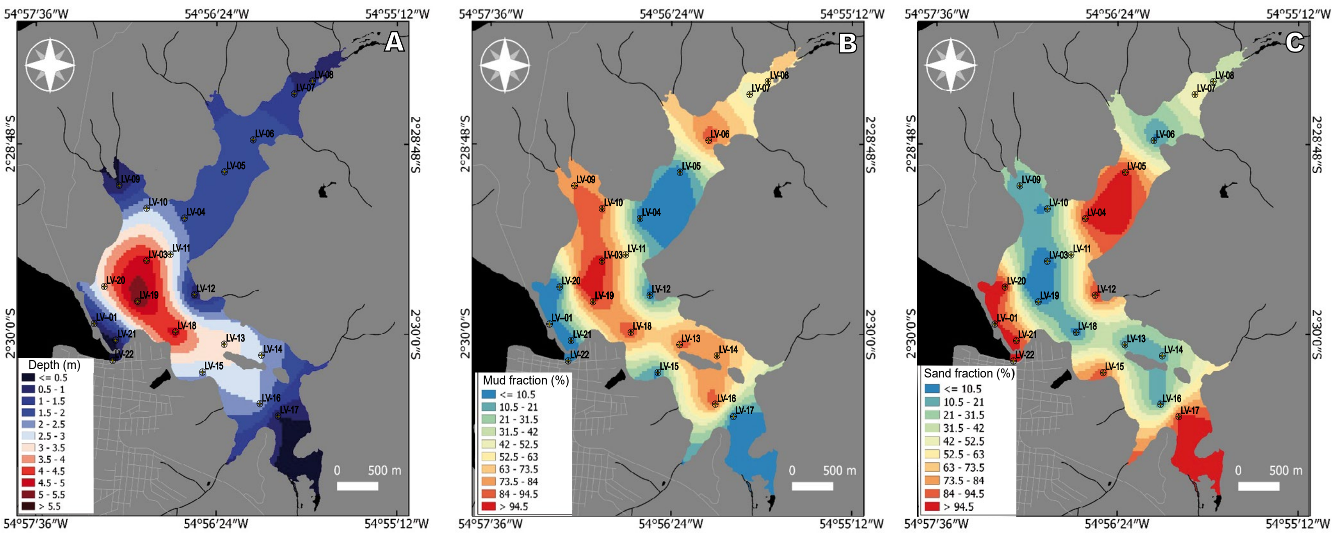


**FIGURE 2.** A) Green Lake bathymetry map, B) sand fraction spatial distribution map and C) mud fraction spatial distribution map. From Mendes *et al.* (2020).

**TABLE 1.** Sample spatial distributions, collection depth and physical properties of Green Lake (LV-19 point), Brazilian Amazon

| Samples | UTM coordinate X | UTM coordinate Y | Depth (m) | Depth (m) | Temperature (°C) | DO ($O_2$ mg.L$^{-1}$) | EC (μS.cm-1) | Turbidity (UNT) | pH |
|---|---|---|---|---|---|---|---|---|---|
| LV-01 | 727526 | 9723610 | 0.5 | 0.2 | 29.5 | 6.10 | 13.16 | 2.10 | 4.05 |
| LV-03 | 728207 | 9724356 | 4.8 | 0.5 | 29.5 | 6.06 | 12.66 | 1.92 | 4.08 |
| LV-04 | 728673 | 9724850 | 1.8 | 1.0 | 29.3 | 6.25 | 12.79 | 1.78 | 4.12 |
| LV-05 | 729165 | 9725390 | 1.8 | 1.5 | 29.3 | 6.17 | 12.53 | 2.31 | 4.15 |
| LV-06 | 729519 | 9725765 | 2 | 2.0 | 29.2 | 6.08 | 12.45 | 1.79 | 4.14 |
| LV-07 | 730030 | 9726300 | 1 | 2.5 | 29.2 | 6.24 | 12.42 | 1.95 | 4.19 |
| LV-08 | 730256 | 9726449 | 1 | 3.0 | 29.1 | 5.87 | 12.67 | 2.17 | 4.16 |
| LV-09 | 727867 | 9725236 | 0.5 | 3.5 | 29.1 | 5.68 | 12.47 | 1.84 | 4.31 |
| LV-10 | 728203 | 9724964 | 2.5 | 4.0 | 29.1 | 5.80 | 12.64 | 1.79 | 4.32 |
| LV-11 | 728497 | 9724430 | 3 | 4.5 | 29.1 | 5.77 | 12.67 | 1.82 | 4.29 |
| LV-12 | 728794 | 9723951 | 0.5 | 5.0 | 29.0 | 5.53 | 12.69 | 2.26 | 4.26 |
| LV-13 | 729164 | 9723381 | 3.5 | 5.5 | 29.0 | 5.81 | 12.59 | 1.90 | 4.23 |
| LV-14 | 729625 | 9723252 | 2.5 | | | | | | |
| LV-15 | 728897 | 9723053 | 2.5 | | | | | | |
| LV-16 | 729602 | 9722686 | 2.5 | | | | | | |
| LV-17 | 729823 | 9722539 | 0.5 | | | | | | |
| LV-18 | 728560 | 9723522 | 4.8 | | | | | | |
| LV-19 | 728101 | 9723878 | 5.5 | | | | | | |
| LV-20 | 727685 | 9724051 | 3.5 | | | | | | |
| LV-21 | 727825 | 9723428 | 0.5 | | | | | | |
| LV-22 | 727789 | 9723192 | 0.2 | | | | | | |

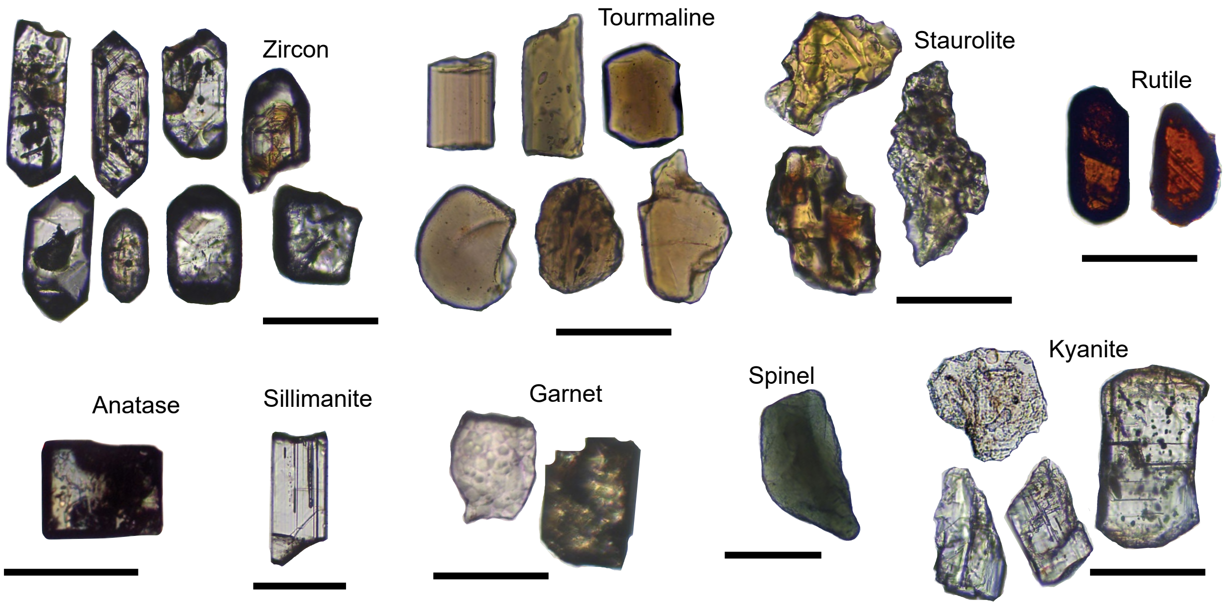


**FIGURE 3.** Photomicrographs of heavy minerals from bottom sediments of Green Lake,Brazil. Scale bars = 0.1mm.

**TABLE 2.** Percentual composition and statistical parameters of transparent and non-micaceous heavy minerals, very-fine sand fraction (63-125µm) from Green Lake bottom sediments. Zir= zircon; Tou= tourmaline; Rut= rutile; Kya= kyanite; Sta= staurolite; Ana= anatase; Sil= sillimanite; Gar= garnet; Spi= spinel; ZTR= Zircon + Tourmaline + Rutile index; S= Standard deviation; CV= Coefficient of variation [SD/mean] x 100; DV= Density variation (g/cm$^3$)

| Sample | Zir | Tou | Rut | kya | Sta | Ana | Sil | Gar | Spi | ZTR |
|---|---|---|---|---|---|---|---|---|---|---|
| LV-01 | 83.5 | 6.0 | 2.0 | 1.5 | 4.0 | 1.0 | 2.0 | 0.0 | 0.0 | 91.5 |
| LV-03 | 86.5 | 4.7 | 2.0 | 2.0 | 2.8 | 1.0 | 1.0 | 0.0 | 0.0 | 93.2 |
| LV-04 | 90.2 | 3.2 | 1.3 | 1.8 | 2.2 | 0.0 | 0.9 | 0.4 | 0.0 | 94.7 |
| LV-05 | 87.3 | 5.9 | 1.0 | 1.0 | 3.0 | 0.8 | 1.0 | 0.0 | 0.0 | 94.2 |
| LV-06 | 83.5 | 7.0 | 1.5 | 2.0 | 3.0 | 1.0 | 1.5 | 0.0 | 0.5 | 92.0 |
| LV-07 | 84.8 | 6.1 | 1.5 | 3.0 | 3.0 | 0.3 | 1.0 | 0.3 | 0.0 | 92.4 |
| LV-08 | 83.5 | 7.5 | 2.0 | 2.5 | 3.5 | 0.0 | 1.0 | 0.0 | 0.0 | 93.0 |
| LV-09 | 87.2 | 4.4 | 0.5 | 2.9 | 3.0 | 0.5 | 1.0 | 0.0 | 0.5 | 92.1 |
| LV-10 | 88.0 | 4.0 | 1.0 | 2.5 | 3.5 | 0.0 | 1.0 | 0.0 | 0.0 | 93.0 |
| LV-11 | 86.5 | 4.0 | 1.0 | 2.5 | 4.0 | 0.5 | 1.5 | 0.0 | 0.0 | 91.5 |
| LV-12 | 88.8 | 7.1 | 0.9 | 1.7 | 0.5 | 0.0 | 0.5 | 0.0 | 0.5 | 96.8 |
| LV-13 | 83.8 | 7.6 | 1.5 | 2.3 | 1.9 | 1.0 | 1.9 | 0.0 | 0.0 | 92.9 |
| LV-14 | 82.0 | 10.5 | 1.0 | 2.5 | 2.0 | 0.5 | 1.5 | 0.0 | 0.0 | 93.5 |
| LV-15 | 90.2 | 6.3 | 0.5 | 1.5 | 1.0 | 0.0 | 0.5 | 0.0 | 0.0 | 97.0 |
| LV-16 | 83.0 | 9.5 | 1.0 | 2.0 | 1.5 | 1.5 | 1.5 | 0.0 | 0.0 | 93.5 |
| LV-17 | 68.1 | 22.2 | 0.5 | 1.8 | 6.4 | 0.0 | 0.5 | 0.0 | 0.5 | 90.8 |
| LV-18 | 79.0 | 12.0 | 1.5 | 3.0 | 3.5 | 0.0 | 1.0 | 0.0 | 0.0 | 92.5 |
| LV-19 | 77.5 | 13.0 | 0.5 | 2.5 | 5.0 | 0.0 | 1.5 | 0.0 | 0.0 | 91.0 |
| LV-20 | 79.0 | 12.5 | 1.0 | 2.0 | 5.0 | 0.0 | 0.5 | 0.0 | 0.0 | 92.5 |
| LV-21 | 77.5 | 15.0 | 1.0 | 1.0 | 5.0 | 0.0 | 0.5 | 0.0 | 0.0 | 93.5 |
| LV-22 | 89.1 | 4.2 | 3.2 | 1.0 | 1.5 | 0.0 | 1.0 | 0.0 | 0.0 | 96.5 |
| Min | 68.1 | 3.2 | 0.5 | 1.0 | 0.5 | 0.0 | 0.5 | 0.0 | 0.0 | 90.8 |
| Max | 90.2 | 22.2 | 3.2 | 3.0 | 6.4 | 1.5 | 2.0 | 0.4 | 0.5 | 97.0 |
| Mean | 83.8 | 8.2 | 1.3 | 2.0 | 3.1 | 0.4 | 1.1 | 0.0 | 0.1 | 93.2 |
| SD | 5.3 | 4.6 | 0.7 | 0.6 | 1.5 | 0.5 | 0.5 | 0.1 | 0.2 | 1.8 |
| CV (%) | 6.3 | 56.1 | 53.8 | 30.0 | 48.4 | 125.0 | 45.5 | 0.0 | 200.0 | 1.9 |
| DV | 4.6 – 4.7 | 2.9 – 3.4 | 4.18 –4.25 | 3.5 – 3.65 | 3.6 – 3.8 | 3.8 – 3.97 | 3.23 –3.27 | 3.4 – 4.3 | 3.5 – 4.1 | |

## Multivariate Statistical Analyses

### *Correlation analysis*

Pearson correlation coefficient (r) indicates that only some of the heavy mineral pairs are correlated (Table 3). The statistically significant pairs (P< 0.01) are delineated and have positive correlation values. Zircon -tourmaline and zircon- staurolite are negatively correlated (-0.947 and -0.775, respectively), while tourmaline -staurolite and sillimanite- anatase show positive correlations (0.628 and 0.675, respectively). The correlations for the other mineral pairs are not significant.

### *Principal components analysis*

Due to the complexity of correlation results (positive and negative), we have performed PCA additional analyses on heavy minerals to aid in delineating their provenance.

By extracting eigenvectors and eigenvalues from the correlation matrix, the number of main significant components and the percentage of total variance they explain (Table 4) were determined. Four statistically significant components explain 79.6% of the total variance obtained by the linear discriminant function equations (Table 5). Opaque, mica, and authigenic minerals were excluded from the linear discriminant calculation. The four eigenvectors present values greater than 1 and the first two represent 53% of the total variance. It indicates that these two eigenvectors are the most important and capable of discriminating the studied sediments.

The first eigenvector constituted 33.8% of the total variance and presented greater weights for zircon, tourmaline,

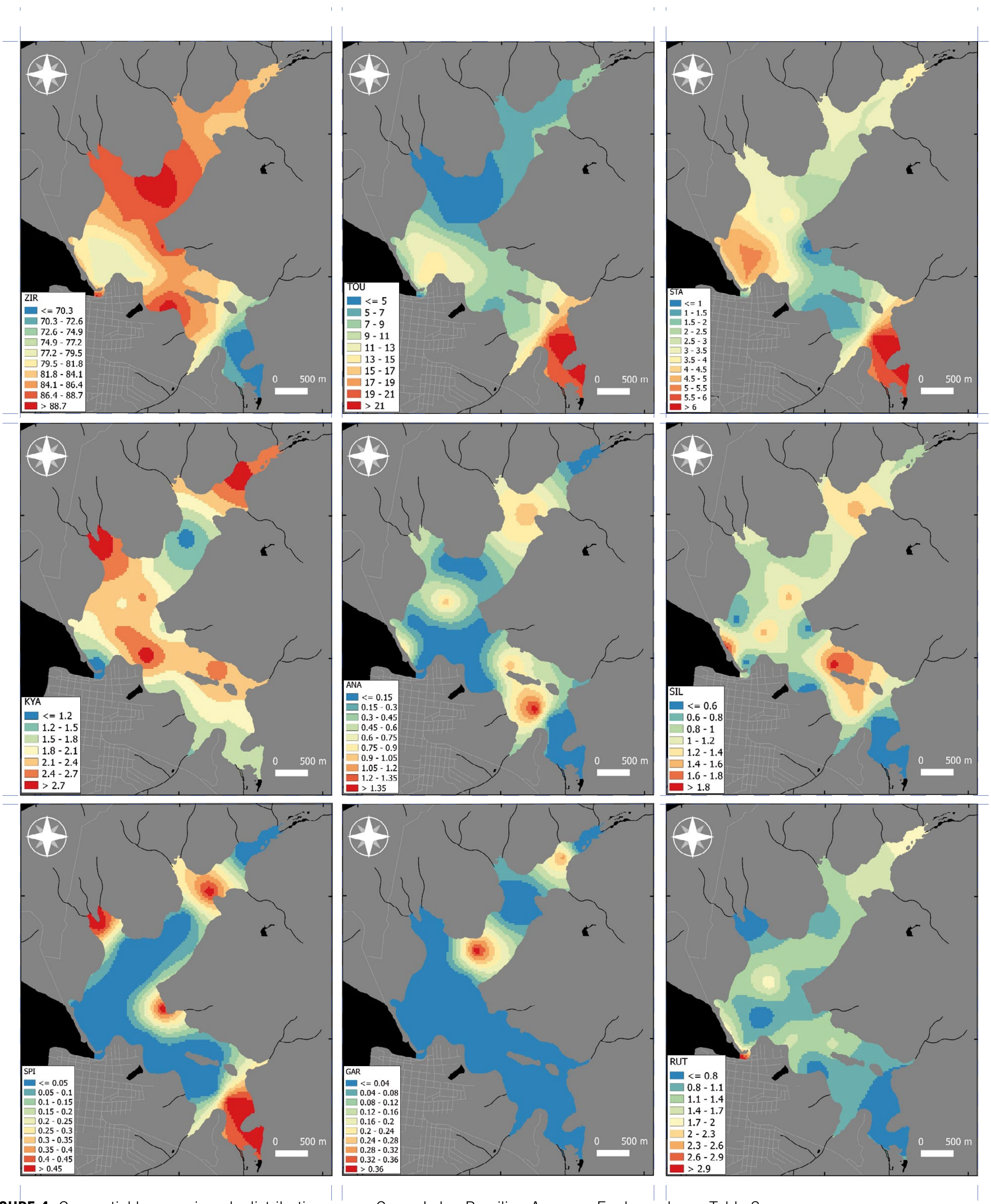


**FIGURE 4.** Geospatial heavy minerals distribution maps, Green Lake, Brazilian Amazon. For legend, see Table 2.

and staurolite. The second eigenvector presented 18.77% of the total variance and the greatest weights are for anatase and sillimanite. The third eigenvector constituted 13.7% of the total variance and presented the greatest weights for rutile and spinel. The fourth eigenvector explained 13.2% of the total variance and presented the greatest weights for kyanite and garnet.

The communality values above 0.6 indicate that the number of factors is acceptable and validates the factor

**TABLE 3.** The Pearson's correlation coefficient (r) matrix for the relationships among the concentrations of the nine heavy minerals, Green Lake, Alter do Chão Village

| | Zircon | Tourmaline | Rutile | kyanite | Staurolite | Anatase | Sillimanite | Garnet | Spinel |
|---|---|---|---|---|---|---|---|---|---|
| Zircon | 1.000 | -0.947 | 0.279 | -0.100 | -0.775 | 0.126 | 0.074 | 0.254 | -0.174 |
| Tourmaline | | 1.000 | -0.385 | -0.049 | 0.628 | -0.249 | -0.280 | -0.268 | 0.209 |
| Rutile | | | 1.000 | -0.207 | -0.237 | 0.130 | 0.253 | 0.065 | -0.309 |
| kyanite | | | | 1.000 | 0.097 | -0.023 | 0.256 | 0.141 | 0.042 |
| Staurolite | | | | | 1.000 | -0.242 | -0.097 | -0.126 | 0.039 |
| Anatase | | | | | | 1.000 | 0.675 | -0.176 | -0.011 |
| Sillimanite | | | | | | | 1.000 | -0.103 | -0.229 |
| Garnet | | | | | | | | 1.000 | -0.156 |
| Spinel | | | | | | | | | 1.000 |

model used (Hair Jr. *et al.*, 2014). A principal component plotting was performed (Fig. 5). In the 2D plot, the tourmaline-staurolite and sillimanite-anatase pairs have an opposite direction relative to zircon (Fig. 5A). In the 3D plot, three relationships were made with Kya-Spi-Sta-Tou; Gar-Rut-Sil-Ana and Zir (Fig. 5B).

*Cluster analysis*

The heavy mineral values were standardized using z-scores and the Euclidian distances between the heavy mineral values were calculated. The hierarchical cluster grouping is presented as a dendrogram. The dendrogram indicates the existence of three subgroups: the first one contains only zircon; the second one contains tourmaline, kyanite, spinel, and staurolite; and the third one contains garnet, rutile, anatase, sillimanite (Fig. 5C).

## DISCUSSION

The grain size of the Green Lake sediments varies between mud and coarse sand (Mendes *et al.*, 2020), which is a sedimentary characteristic of Amazonian lakes (Souza-Filho *et al.*, 2016). To determine the spatial distribution of heavy minerals, the application of classical and modern analytical techniques was required. In addition, distribution modeling was applied to understand changes in provenance, morphological characteristics, control during transportation, and recent or past climates (Morton and Hallsworth, 1994, 1999).

The geostatistical and multivariate statistical techniques are efficient tools for identifying distribution patterns of the heavy mineral assemblage of the Green Lake and assessing the sediment source. Despite their efficiency, the application of these techniques in heavy minerals studies is uncommon (Derkachev and Nikolaeva, 2007; Ochoa *et al.*, 2013; Ryan *et al.*, 2007). PCA has been widely used in a variety of studies to reduce the number of parameters and facilitate correlation analysis between variables (Tokalıoğlu and Kartal, 2006). The kriging grouping (Fig. 4) combined with PCA assisted in determining the main heavy minerals groups and in interpreting the sediments source.

In this work, it was assumed that a significant positive correlation between heavy mineral pairs (Tour-Sta, Sil-Ana)

**TABLE 4.** Principal Components Analysis (PCA) results of heavy mineral concentrations of Green Lake after varimax rotation with Kaiser normalization

| Mineral | Principal component | | | | Communalities |
|---|---|---|---|---|---|
| | 1 | 2 | 3 | 4 | |
| Zircon | -0.966 | -0.017 | 0.135 | 0.005 | 0.952 |
| Tourmaline | 0.890 | -0.160 | -0.238 | -0.141 | 0.894 |
| Rutile | -0.265 | 0.158 | 0.684 | -0.278 | 0.641 |
| kyanite | 0.087 | 0.186 | -0.158 | 0.872 | 0.828 |
| Staurolite | 0.869 | -0.105 | 0.046 | 0.109 | 0.781 |
| Anatase | -0.183 | 0.871 | -0.022 | -0.087 | 0.800 |
| Sillimanite | -0.053 | 0.874 | 0.267 | 0.231 | 0.891 |
| Garnet | -0.297 | -0.416 | 0.289 | 0.547 | 0.644 |
| Spinel | 0.006 | -0.028 | -0.852 | -0.101 | 0.736 |
| Initial eigenvalues | 3.048 | 1.689 | 1.238 | 1.193 | |
| Variance (%) | 33.868 | 18.771 | 13.756 | 13.250 | |
| Cumulative variance (%) | 33.868 | 52.639 | 66.395 | 79.645 | |

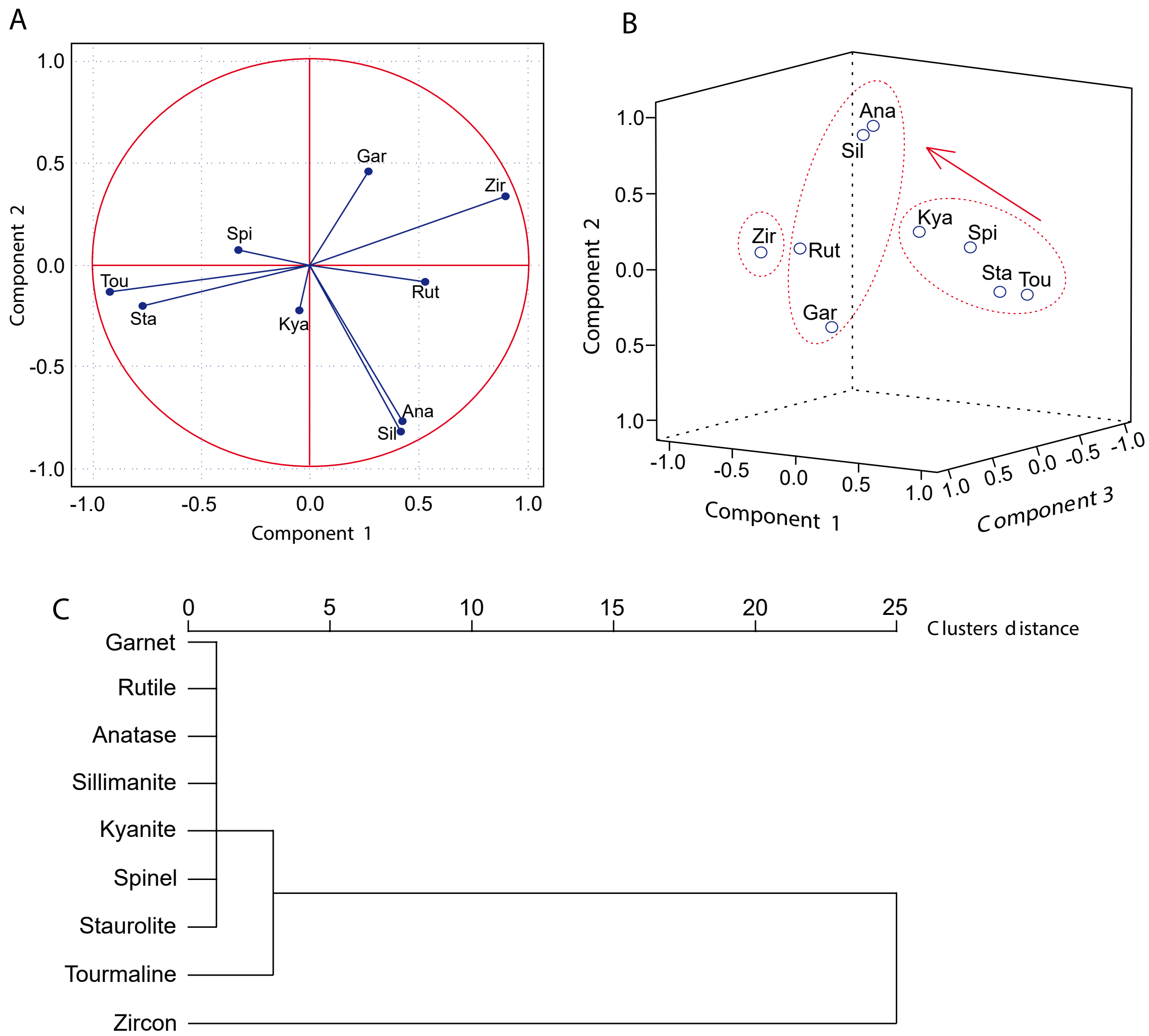


**FIGURE 5.** Principal Components Analysis (PCA) loadings for the principal components for the heavy minerals study. A) 2-D plotting of the two principal components (PC1 vs. PC2); B) 3-D plotting of the three principal components (PC1 vs. PC2 vs. PC3) for the nine heavy minerals under study. Details are shown in Tables 3 and 4. The red arrow indicates metamorphic degree increase; C) hierarchical dendrogram of the heavy minerals using Ward's clustering method.

suggests a common or combined source, and a negative correlation (Zir-Tou, Zir-Sta) suggests mixing of sources. The other mineral correlations (Kya, Rut, Gar, Spi) are not well defined.

The results of this study suggest that the Green Lake heavy minerals can be classified into three groups (Tables 3; 4; Figs. 4; 5): Group 1 (Tou–Sta–Spi-Kya), Group 2 (Gar–Rut–Sil-Ana), and Group 3 (Zir). This classification indicates that the sediments are from at least two different rock types: metamorphic rocks, Groups 1 and 2, and acid igneous rocks, Group 3. Based on the PCA analysis (Table 4), internal variations were associated with the degree of metamorphism (Fig. 5B). Despite the metamorphic origin, temperature and pressure variations in the minerals' formation reflect stability of the minerals under the weathering conditions.

Variations in the degree of correlation in Groups 1 and 2 indicate changes from medium to high-grade metamorphic source rock types. The occurrence of kyanite and sillimanite indicate metapelites as source rock because they are rich in aluminum (Winter, 2014). Minerals in Group 1 show significant correlation indicating medium-grade metamorphic rocks as common source. Generally, these metamorphic minerals are common in schists, meta-schists, and gneisses (Deer *et al.*, 1997). Group 2 minerals are common in high-grade metamorphic rocks. Group 3, composed by zircon only, did not have a significant correlation with any other group, suggesting their source is different from Group 1 and 2.

**TABLE 5.** Linear discriminant function equations used for separation of mineral groups. For legend, see Table 2

$$df_1 = -0.966zir + 0.890tou - 0.265rut + 0.087kya + 0.869sta - 0.183ana - 0.053sil - 0.297gar + 0.006spi$$

$$df_2 = -0.017zir - 0.160tou + 0.158rut + 0.186kya - 0.105sta + 0.871ana + 0.874sil - 0.416gar - 0.028spi$$

$$df_3 = +0.135zir - 0.238tou + 0.684rut - 0.158kya + 0.046sta - 0.022ana + 0.267sil + 0.289gar - 0.852spi$$

$$df_4 = +0.005zir - 0.141tou - 0.278rut + 0.872kya + 0.109sta - 0.087ana + 0.231sil + 0.547gar - 0.101spi$$

Three possibilities are proposed to explain the variations and spatial distribution of the Green Lake heavy minerals: i) fluvial dynamic interaction between the Tapajós River and the Amazon River; ii) internal dynamics of the lake related to the physicochemical variables and iii) variations in the source of the sediments.

Due to its higher discharge, the Amazon River flows into the Tapajós River (Freitas *et al.*, 2017; Medeiros Filho, 2015; Medeiros Filho *et al.*, 2016), and, thus, it may introduce sediments into the Green Lake. However, the immature heavy mineral assemblage of the Amazon River is mainly composed of hypersthene, augite, and amphibole derived from Andean source rocks (Landim *et al.*, 1983; Lima Jr. and Nogueira, 2013). This assemblage differs from the Green Lake heavy mineral assemblage in terms of mineral species and mineral proportion. Therefore, the possibility of the Amazon River controlling the Green Lake heavy mineral assemblage was disregarded.

Hydrographic studies on the Tapajós River have been focused on physical-chemical analyses (Sousa *et al.*, 2009), heavy metals (Maia *et al.*, 2016), carbon content (Bertassoli Jr. *et al.*, 2017) and description of heavy mineral assemblages (Gozzi, 2019). Despite its the importance, only a few studies on sediment characterization of the Tapajós River have been performed (Medeiros Filho, 2015; Medeiros Filho *et al.*, 2016).

In order to state that the Tapajós River introduces sediments into the Green Lake, it is necessary to demonstrate that the sediment dispersal pattern in the lake is controlled by the Tapajós River. This relationship is well-defined during the Amazonian winter when the Tapajós River flows into the Green Lake (Fig. 1F), and the Amazonian summer, when Green Lake is isolated from the Tapajós River (Fig. 1E). However, sediment transport of Tapajós River is hampered by the hydraulic-barrier effect in the confluence of Tapajós and Amazon rivers (Nascimento *et al.*, 1976).

Provenance studies at the confluence of the Madeira and Amazon rivers suggest that the Madeira River contributes with heavy minerals derived from a cratonic source and, the Amazon River provides andalusite-rich Andean sediments (Nascimento Jr. *et al.*, 2015). At the Xingu and Amazon rivers confluence, there is a dominance of unstable heavy minerals (epidote, hypersthene, amphibole) whereas upstream along the Xingu River stable/ultra-stable heavy minerals (zircon, tourmaline, rutile) dominate (Souza, 2018). If identical geological context occurs at the Amazon and Tapajós river confluence (Fig.1A), one would expect that the heavy mineral assemblage of the Tapajós River was unstable like the one in the Xingu River, however, this is not the case.

The Tapajós River is characterized by an irregular ultrastable heavy minerals distribution (Gozzi, 2019). Upstream, tourmaline is the dominant constituent (65 to 70%), while zircon registers up to 45%. Downstream, near the Green Lake, rutile (33%) and tourmaline (50%) occur. The Green Lake heavy mineral assemblage is represented by medium to high-grade metamorphic minerals together with igneous minerals (Mendes *et al.*, 2020) (Fig. 3; Table 2).

The species and relative proportions of the Green Lake heavy minerals differ from those downstream of the Tapajós River, so it is unlikely to consider the Tapajós River introduces sediments into the Green Lake. Geospatial distribution of the Green Lake heavy minerals is another evidence the Tapajós River cannot be the source of these sediments. The concentration of the heavy minerals is low in the western and southwestern portions of the lake (Fig. 4), which is where the Tapajós River flows into the lake. Therefore, this low concentration suggests an insignificant heavy minerals transportation into the lake.

Low Zr and Hf values in the Tapajós River, near Alter do Chão and Santarém areas, indicates deposition of zircon grains, which are related to an earlier Green Lake deposit (Medeiros Filho *et al.*, 2016). This is an additional evidence to disregard the Tapajos River as the supplier of sediments to the Green Lake. As the Green Lake heavy mineral assemblage is not similar to that of the Tapajós River, other sedimentary sources were considered.

The area surrounding Green Lake is composed of friable rocks of the Alter do Chão Formation. This formation is known for its siliciclastic composition (conglomerate, sandstones and mudstones). High degree of weathering results in feldspar hydrolysis —a common phenomenon under hot and humid climate conditions like that one in the Amazon region— and kaolinite neoformation (Mendes *et al.*, 2013). The Green Lake heavy mineral assemblage is similar in species and relative concentration to that of the Alter do Chão Formation (Mendes *et al.*, 2013, 2015, 2020).

The Green Lake heavy mineral assemblage is mainly controlled by recent/modern weathering and erosion of the rocks surrounding the lake, the Alter do Chão Formation. This weathering modifies the original mineral assemblage by eliminating less stable heavy minerals. In this case, application of discriminant equations (Table 5) proved to be an important tool to determine the relationship between the heavy mineral assemblage of the Alter do Chão Formation and the one found in the Green Lake.

Low pH values, electrical conductivity, and dissolved oxygen in the Green Lake contribute to the mortality of organisms, thereby, generating carbonic acids which, in turn, increase the corrosion potential. ZTR minerals are not affected by superficially pH conditions and shallow diagenesis, but garnet and spinel, as well as other unstable minerals, are sensitive and easily dissolved in this weathering environment (acid pH) (Morton, 1984). Some of the superficial textures of the heavy mineral grains indicating chemical dissolution in the Green Lake heavy minerals corroborate this interpretation (Mendes *et al.*, 2020).

The recent ultra-stable mineral assemblage of Green Lake (ZTR> 90%) suggests that most of the original minerals were eliminated. This feature is corroborated by the low abundance of unstable minerals in the lake sediments. The heavy mineral dissolution and modification may, to some extent, be responsible for the spatial distribution pattern of heavy minerals in the Green Lake - when only one sediment source is considered.

## CONCLUSIONS

Researches on provenance and spatial distribution of bottom sediments in Amazonian fluvial lakes are rare. This study aims to understand the spatial distribution and source rocks of the Green Lake sediments through geostatistical and multivariate statistical analysis. The Green Lake heavy mineral assemblage demonstrates various spatial distribution patterns. Using PCA and cluster analysis, three heavy mineral groups were identified. Group 1 and 2 suggest sediment contribution from medium to high-grade metamorphic source rocks, while Group 3 suggests sediments originating from acid igneous source rocks. From these results, the authors concluded that the Green Lake bottom sediments come from weathering and erosion of the outcrops of Alter do Chão Formation that are surrounding the lake. The bottom sediments of this lake were not a contribution of either the Tapajós River or the Amazon River. Factors related to the surface weathering of the Amazonian region, pH, dissolved oxygen amounts, and electric conductivity made the Green Lake water acidic. This feature has increased the corrosion potential of the lake water and, hence, caused dissolution of unstable heavy minerals, resulting in their observed geospatial distribution pattern.

## CONFLICT OF INTEREST

On behalf of all authors, the corresponding author states that there is no conflict of interest.

## ACKNOWLEDGMENTS

Grant for this research was provided by the Propesp-UFPA through the “Itaituba Formation Heavy Minerals, central portion of the Amazonas Basin in Pará State” project (PRO1795-2017), and Federal University of Western Pará (UFOPA): 06/2016-PROPPIT/UFOPA-PROFIC grant. The authors are grateful to the Interdisciplinary Group in Applied Geology (GIGA) for discussion, the Federal University of Pará (UFPA) for their laboratory support, and to Dr. Enayatollah Ranjineh Khojasteh, Dr. Parthasarathi Ghosh and Dra. Concha Arenas Abad for their excellent contributions that have been very helpful in improving the manuscript.

## REFERENCES

Agência Nacional de Águas (ANA) Brasil, 2018. Hidroweb: Sistema de Informações Hidrológicas. Available online at: http://www.snirh.gov.br/hidroweb/ Accessed: October 1, 2018.

Aguiar Neto, A.B., Marques, W.S., Freire, G.S.S., 2016. Distribuição espacial de minerais pesados nos sedimentos superficiais da Plataforma Continental Oeste do Ceará, Nordeste do Brasil. Pesquisas em Geociências, 43, 69-83. DOI: https://doi.org/10.22456/1807-9806.78193

Bertassoli Jr., D.J., Sawakuchi, A.O., Sawakuchi, H.O., Pupim, F.N., Hartmann, G.A., McGlue, M.M, Chiessi, C.M., Zabel, M., Schefuß, E., Pereira, T.S., Santos, R.A., Faustino, S.B., Oliveira, P.E., Bicudo, D.C., 2017. The Fate of Carbon in Sediments of the Xingu and Tapajós Clearwater Rivers, Eastern Amazon. Frontiers in Marine Science, 22, 1-14. DOI: https://doi.org/10.3389/fmars.2017.00044

Brito, R.N.R., Asp, N.E., Beasley, C.R., Santos, H.S.S., 2009. Características sedimentares fluviais associadas ao grau de preservação da Mata Ciliar - Rio Urumajó, Nordeste Paraense. Acta Amazônica, 39, 173-180. DOI: https://doi.org/10.1590/S0044-59672009000100017

Carvalho, N.O., 2008. Hidrossedimentologia Prática. Rio de Janeiro, Companhia de Pesquisa em Recursos Minerais (CPRM), 600pp.

Cascalho, J., 2019. Provenance of Heavy Minerals: A Case Study from the WNW Portuguese Continental Margin. Minerals, 9, 355-388. DOI: https://doi.org/10.3390/min9060355

Dadalto, T.P., Albino, J., 2009. Morphotextural analysis and application of sediment transportation models in submerged area adjacent to an artificial beach in erosive process. Quaternary and Environmental Geosciences, 1, 16-24. DOI: http://dx.doi.org/10.5380/abequa.v1i1.14189

Deer, W.A., Howie, R.A., Zussman, J., 1997. Rock-forming Minerals vol. 1A, Orthosilicates. London (UK), The Geological Society, 936pp.

Derkachev, A.N, Nikolaeva, N.A., 2007. Multivariate analysis of heavy mineral assemblages of sediments from the marginal seas of the Western Pacific. In: Mange, M.A., Wright, D.T. (eds.). Heavy Minerals in Use. Developments in Sedimentology, 58, 439-464.

Ebqa'ai, M., Ibrahim, B., 2017. Application of multivariate statistical analysis in the pollution and health risk of traffic-related heavy metals. Environment Geochemistry Health, 39, 1441-1456. DOI: https://doi.org/10.1007/s10653-017-9930-9

Freitas, P.T.A., Asp, N.E., Souza-Filho, P.W.M., Nittrouer, C.A., Ogston, A.S., Silva, M. S., 2017. Tidal influence on the hydrodynamics and sediment entrapment in a major Amazon River tributary – Lower Tapajós River. Journal of South American Earth Sciences, 79, 189-201. DOI: 10.1016/j.jsames.2017.08.005

Frihy, O.E., Deabes, E.A., Abudia, A.A., Adawi, A., 2022. Heavy mineral composition and texture of the recently formed fluvial delta sediment of Lake Nasser/Nubia, Egypt and Sudan. International Journal of Sediment Research, 37, 70-82. DOI: https://doi.org/10.1016/j.ijsrc.2021.07.002

Galehouse, J.S., 1971. Sedimentation analysis. In: Carver, R.R. (ed.). Procedures in Sedimentary Petrology, New York, Wiley-Interscience, 69-94.

Góes, A.M., Rossetti, D.F., Mendes, A.C., 2007. Heavy mineral as a tool to refine the stratigraphy of kaolin deposits in the Rio Capim Area, Northern Brazil. Anais da Academia Brasileira de Ciências, 79, 457-471. DOI: https://doi.org/10.1590/S0001-37652007000300009

Gozzi, P.V.T., 2019. Mineralogia e geoquímica dos sedimentos de fundo do rio-lago Tapajós-PA. Master's Thesis. Belém, Federal University of Pará, 1-106.

Guyot, J.L., Jouanneau, J.M., Soares, L., Boaventura, G.R., Maillet, N., Lagane, C., 2007. Clay mineral composition of river sediments in the Amazon Basin. Catena, 71, 340-356. DOI: https://doi.org/10.1016/j.catena.2007.02.002

Hair Jr., J.F., Black, W.C., Babin, B.J., Anderson, R.E., 2014. Multivariate Data Analysis. British Library Cataloguing-in-Publication Data, 739pp.

Hubert, J.E., 1962. A zircon-tourmaline-rutile maturity index and the interdependence of the composition of heavy mineral assemblages with the cross composition and texture of sandstones. Journal of Sedimentary Petrolology, 32, 440-450. DOI: http://dx.doi.org/10.1306/74D70CE5-2B21-11D7-8648000102C1865D

Knox, R.W.O'B., Franks, S.G., Cocker, J.D., 2007. Stratigraphic evolution of heavy-mineral provenance signatures in the sandstones of the Wajid Group (Cambrian to Permian), southwestern Saudi Arabia. GeoArabia, 12, 65-96.

Landim, P.M.B., Bósio, N.J., Wu, F.T., Castro, P.R.M., 1983. Minerais pesados provenientes do leio do rio Amazonas. Acta Amazônica, 13, 51-72. DOI: https://doi.org/10.1590/1809-43921983131051

Leandro, G.R.S., Souza, C.A., Nascimento, F.R., 2014. Bottom sediments and in suspension in fluvial corridor of the Paraguay River, north Pantanal of Mato Grosso, Brazil. Boletim Goiano de Geografia, 34, 195-214.

Lima Jr., W.J.S., Nogueira, A.C.R., 2013. Sedimentologia e proveniência de depósitos recentes do rio Amazonas, entre Santarém (PA) e Macapá (AP). Belém (PA), 13° Simpósio de Geologia da Amazônia (Cd-Rom).

Lu, X., Wang, L., Li, L.Y., Lei, K., Huang, L., Kang, D., 2010. Multivariate statistical analysis of heavy metals in street dust of Baoji, NW China. Journal of Hazardous Materials, 173, 744-749. DOI: https://doi.org/10.1016/j.jhazmat.2009.09.001

Maia, A.R., Peleja, J.R.P., Goch, Y.G.F., Bacelar, R., Souza, D.A., Lemos, E.J.S., 2016. Mercúrio total em sedimentos fluviais da Bacia do rio Tapajós em regiões com e sem atividade garimpeira. Amazônia, Brasil. In: Ecotox. Curitiba (PR), Brazil, XVI Congresso Brasileiro de Ecotoxicologia, 607-609.

Matiatos, I., 2016. Nitrate source identification in groundwater of multiple land-use areas by combining isotopes and multivariate statistical analysis: A case study of Asopos basin (Central Greece). Science of the Total Environment, 541, 802-814. DOI: https://doi.org/10.1016/j.scitotenv.2015.09.134

Meade, R.H., Rayol, J.M., Conceição, S.C., Natividade, J.R.G., 1991. Backwater effects in the Amazon River Basin of Brazil. Environmental Geology and Water Sciences, 18, 105-114. DOI: https://doi.org/10.1007/BF01704664

Medeiros Filho, L.C., 2015. Influência do Rio Amazonas nos sedimentos de fundo do baixo Rio Tapajós: evidências geoquímicas e isotópicas (Pb-Sr-Nd). Master's Thesis. Belém, Federal University of Pará, 1-93.

Medeiros Filho, L.C., Lafon, J.M., Souza-Filho, P.W.M., 2016. Pb-Sr-Nd isotopic tracing of the influence of the Amazon River on the bottom sediments in the lower Tapajós River. Journal of South American Earth Scienc-es, 70, 36-48. DOI: https://doi.org/10.1016/j.jsames.2016.04.012

Mendes, A.C., Santos Júnior, A.E.A., Nogueira, A.C.R., 2013. Petrografia de arenitos e minerais pesados da Formação Alter

do Chão, bacia do Amazonas. Belém (PA), 13° Simpósio de Geologia da Amazônia (Cd-Rom).
Mendes, A.C., Salomão, G.N., Nogueira, A.C.R., Dantas, E.L., 2015. Provenance of the Alter do Chão Formation in Amazonas State (Itacoatiara-Parintins cities), Amazonas Basin, Brazil. Brasília, XV Congresso Brasileiro de Geoquímica and International Symposium on Climate and Geodynamics of Amazon Basin (Cd-Rom).
Mendes, A.C., Dantas, A.B., Ribeiro, A.C.S., Santos, L.O., Mendes, K.C., Moraes, D S. Almeida, R.M., 2020. Provenance of heavy and clay minerals in bottom sediments of Green Lake, an Amazonian fluvial lake in Brazil. Acta Amazonica, 50, 159-169. DOI: https://doi.org/10.1590/1809-4392201804681
Moquet, J.S., Guyot, J.L., Crave, A., Viers, J., Filizola, N., Martinez, J.M., Oliveira, T.C. S., Sánchez, L.S.H., Lagane, C., Lavado, W., Noriega, L., Pombosa, R., 2016. Amazon River dissolved load: temporal dynamics and annual budget from the Andes to the ocean. Environmental Science and Pollution Research, 23, 11405-11429. DOI: https://doi.org/10.1007/s11356-015-5503-6
Moral Cardona, J.P., Gutiérrez Mas, J.M., Sánchez Bellón, A., Domínguez-Bella, S., Martínez López, J., 2005. Surface textures of heavy-mineral grains: a new contribution to provenance studies. Sedimentary Geology, 174, 223-235. DOI: https://doi.org/10.1016/j.sedgeo.2004.12.006
Morton. A.C., 1984. Stability of detrital heavy minerals in Tertiary sandstones from the North Sea Basin. Clay Minerals, 19, 287-308. DOI: https://doi.org/10.1180/claymin.1984.019.3.04
Morton, A.C., Hallsworth, C., 1994. Identifying provenience-specific features of detrital heavy mineral assemblages in sandstones. Sedimentary Geology, 90, 241-256. DOI: https://doi.org/10.1016/0037-0738(94)90041-8
Morton, A.C, Hallsworth, C., 1999. Processes controlling the composition of heavy mineral assemblages in sandstones. Sedimentary Geology, 124, 3-29. DOI: https://doi.org/10.1016/S0037-0738(98)00118-3
Nascimento, D.A., Garcia, M.G.L., Mauro, C.A., 1976. Projeto Radam Brasil. Folha SA.21–Santarém: geologia, geomorfologia, pedologia, vegetação e uso potencial da terra. Rio de Janeiro, Departamento Nacional da Produção Mineral, 10, 132-181.
Nascimento Jr., D.R., Sawakuchi, A.O., Guedes, C.C.F., Giannini, P.C.F., Grohmann, C.H., Ferreira, M.P., 2015. Provenance of sands from the confluence of the Amazon and Madeira rivers based on detrital heavy minerals and luminescence of quartz and feldspar. Sedimentary Geology, 316, 1-12. DOI: https://doi.org/10.1016/j.sedgeo.2014.11.002
Nascimento Jr., D.R., Tossi, L.N.C., Oliveira, V.F., Lucena, B.B., 2017. Morphodynamics, transport and provenance of the recent beach-foredune system between Itarema and Camocim, West Coast of Ceará State (Brazil). Quaternary and Environmental Geosciences, 8, 24-45.
Ochoa, F.L., Góes, A.M., Rossetti, D.F., Sawakuchi, A.O., Cassini, L.V., Coutinho, J.M.V., 2013. Discrimination of Cenozoic deposits from the onshore portion of the Paraíba Basin (NE, Brazil) using heavy minerals and grain size. Brazilian Journal of Geology, 43, 555-570. DOI: https://doi.org/10.5327/Z2317-48892013000300010
Pan, B., Pang, H., Gao, H., Garzanti, E., Zou, Y., Liu, X., Li, F., Jia, Y., 2016. Heavy-mineral analysis and provenance of Yellow River sediments around the China Loess Plateau. Journal of Asian Earth Sciences, 127, 1-11. DOI: https://doi.org/10.1016/j.jseaes.2016.06.006
Ribeiro, A.C.S., Mendes, A.C., Dantas, A.B., Santos, L.O., 2017. Heavy minerals distribution of Green Lake, Alter do Chão Village, Pará State. Foz do Iguaçu (PR), II Congresso Internacional de Hidrossedimentologia, 19-22.
Ryan, P.D., Mange, M.A., Dewey, J.F., 2007. Statistical analysis of high-resolution heavy mineral stratigraphic data from the Ordovician of western Ireland and its tectonic consequences. In: Mange, M.A., Wright, D.T. (eds.). Heavy Minerals in Use. Developments in Sedimentology, 58, 465-490.
Sawakuchi, A.O., Jain, M., Mineli, T.D., Nogueira, L., Bertassoli Jr., D.J., Häggi, C., Sawakuchi, H.O., Pupim, F.N., Grohmann, C.H., Chiessi, C.M., Zabel, M., Mulitza, S., Mazoca, C.E.M., Cunha, D.F., 2018. Luminescence of quartz and feldspar fingerprints provenance and correlates with the source area denudation in the Amazon River basin. Earth and Planetary Science Letters, 492, 152-162. DOI: https://doi.org/10.1016/j.epsl.2018.04.006
Sousa, D.R., Cabral, A.S., Nobre, D., Lobato, H., Goch, Y.G.F., Peleja, J.R.P., Cabral, W.S., 2009. Diagnóstico sedimentar e físico-químico dos igarapés no trecho de Santarém a vila balneária de Alter do Chão-PA. Revista em Foco, 11, 75-85.
Sousa, S.S.C.G., Castro, J.W.A., Guedes, E., 2017. Grain size and heavy minerals of northern Rio de Janeiro state beaches (SE Brazil): sediment distribution and deposition conditions. Geociências, 36, 365-380.
Souza, T.P., 2018. Influência do Rio Amazonas nos sedimentos de fundo do Rio Xingu: evidências mineralógicas e geoquímicas. Master’s Thesis. Belém, Federal University of Pará, 1-115.
Souza-Filho, P.W., Guimarães, J.T.F., Silva, M., Costa, F.R., Sahoo, P.K., Maurity, C., Dall’Agnol, R., 2016. Basin morphology, sedimentology and seismic stratigraphy of an upland lake from Serra dos Carajás, southeastern Amazon, Brazil. Boletim Museu Paraense Emílio Goeldi, Ciências Naturais, 11, 71-83.
Svendsen, J.B., Hartley, N.R., 2002. Synthetic heavy mineral stratigraphy: applications and limitations. Marine and Petroleum Geology, 19, 389-405. DOI: https://doi.org/10.1016/S0264-8172(02)00010-7
Tassinari, C.C.G., Bittencourt, J.S., Geraldes, M.C., Macambira, M.J.B., Lafon, J.M., 2000. The Amazon Craton. In: Cordani, U.G., Thomaz-Filho, A., Campos, D.A. (eds.). Tectonic Evolution of South America. Academia Brasileira de Ciências, Special Publication, 41-95.
Tavares, A.C.A., Bulhões, E., Estrada, A.F.D., 2010. Distribuição de fácies sedimentares e tendências de transporte de sedimentos na enseada de Manguinhos, Armação dos Búzios, RJ. Revista de Geografia, 2, 81-97.

Tokalıoğlu, S., Kartal, S., 2006. Statistical evaluation of the bioavailability of heavy metals from contaminated soils to vegetables. Bulletin of Environmental Contamination and Toxicology, 76, 311-319. DOI: https://doi.org/10.1007/s00128-006-0923-0

Veronez Jr., P., Bastos, A.C., Quaresma, V.S., 2009. Morfologia e distribuição sedimentar em um sistema estuarino tropical: Baia de Vitoria, ES. Revista Brasileira de Geofísica, 27, 609-624. DOI: https://doi.org/10.1590/S0102-261X2009000400006

Vieira, S.R., 2000. Geoestatística em estudos de variabilidade espacial do solo. In: Novais, R.F., Alvarez, V.H., Schaefer, G.R. (eds.). Tópicos em ciência do solo. Viçosa, Sociedade Brasileira de Ciência do Solo, 1-54.

Viers, J., Roddaz, M., Filizola, N., Guyot, J.L., Sondag, F., Brunet, P., Zouiten, C., Boucayrand, C., Martin, F., Boaventura, G.R., 2008. Seasonal and provenance controls on Nd–Sr isotopic compositions of Amazon rivers supended sediments and implications for Nd and Sr fluxes exported to the Atlantic Ocean. Earth and Planetary Science Letters, 274, 511-523. DOI: https://doi.org/10.1016/j.epsl.2008.08.011

Winter, J.D., 2014. A Classification of Metamorphic Rocks. In: Winter, J.D. (ed.). Principles of Igneous and Metamorphic Petrology. Harlow (England), Pearson Education Limited, 491-498.

Wittmann, H., von Blanckenburg, F., Maurice, L., Guyot, J.L., Filizola Jr., N., Kubik, P.W., 2011. Sediment production and delivery in the Amazon River basin quantified by in situ-produced cosmogenic nuclides and recent river loads. Geological Society of America Bulletin, 123, 934-950. DOI: https://doi.org/10.1130/B30317.1

Yang, S., Wang, Z., Guo, Y., Li, C., Cai, J., 2009. Heavy mineral compositions of the Changjiang (Yangtze River) sediments and their provenance-tracing implication. Journal of Asian Earth Sciences, 35, 56-65. DOI: https://doi.org/10.1016/j.jseaes.2008.12.002

Yıldırım, G., Tokalıoğlu, S., 2016. Heavy metal speciation in various grain sizes of industrially contaminated street dust using multivariate statistical analysis. Ecotoxicology and Environmental Safety, 124, 369-376. DOI: https://doi.org/10.1016/j.ecoenv.2015.11.006

Yongming, H., Peixuan, D., Junji, C., Posmentier, E.S., 2006. Multivariate analysis of heavy metal contamination in urban dusts of Xi'an, Central China. Science of the Total Environment, 355, 176-186. DOI: https://doi.org/10.1016/j.scitotenv.2005.02.026

**Manuscript received October 2021;**
**revision accepted April 2022;**
**published Online June 2022.**